

Studies of $[\text{Ag}(\text{PPh}_3)_2]\text{NO}_3$, $[\text{Ag}\{\text{P}(\text{CH}_2\text{CH}_2\text{CN})_3\}_2]\text{NO}_3$ and $[\text{Ag}\{\text{P}(\text{C}_6\text{H}_4\text{Me-}m)_3\}_2]\text{NO}_3$ by X-Ray Diffraction and Solid-state Nuclear Magnetic Resonance†

C. W. Liu,^a Hongjun Pan,^a John P. Fackler, jun.,^{*a} Gang Wu,^b Roderick E. Wasylshen^b and Maoyu Shang^c

^a Department of Chemistry, and Laboratory for Molecular Structure and Bonding, Texas A & M University, College Station, TX 77843-3255, USA

^b Department of Chemistry, Dalhousie University, Halifax, Nova Scotia B3H 4J3, Canada

^c Department of Chemistry, University of Notre Dame, Notre Dame, Indiana 46556, USA

Solid-state magic angle spinning (MAS) ^{31}P NMR spectra of $[\text{Ag}(\text{PPh}_3)_2]\text{NO}_3$ **1**, $[\text{Ag}\{\text{P}(\text{CH}_2\text{CH}_2\text{CN})_3\}_2]\text{NO}_3$ **2** and $[\text{Ag}\{\text{P}(\text{C}_6\text{H}_4\text{Me-}m)_3\}_2]\text{NO}_3$ **3** have been obtained. In addition, the crystal structures for **2** and **3** have been determined. The results from the high-resolution NMR study are consistent with the known structure of **1** and the structures of **2** and **3**. In each case the ^{31}P NMR spectra exhibit resolved splittings arising from ^{107}Ag and ^{109}Ag with $^1J(^{109}\text{Ag}^{31}\text{P})$ values of 524, 564 and 517 Hz for **1**, **2** and **3**, respectively. In **1** the two phosphorus nuclei are crystallographically non-equivalent, thus analysis of the ^{31}P NMR spectrum indicates two chemically shifted phosphorus nuclei, δ_a 9.50 and δ_b 7.67, with $^2J(^{31}\text{P}_A^{31}\text{P}_B) = 125$ Hz. The two phosphorus nuclei of **2** are crystallographically and magnetically equivalent in the solid state as evident from the cross polarization/MAS ^{31}P NMR spectrum, δ -9.56. Crystals of **2** are trigonal, space group $R\bar{3}c$ $a = 12.204(2)$, $c = 26.418(5)$ Å, $Z = 6$. The Ag and P atoms are located on a three-fold rotation axis with Ag at the centre of inversion. The Ag-P bond distance is 2.383(1) Å. The conformation of the cyanoethylphosphine ligands in **2** is analogous to the ribs of an umbrella in which the silver atom is encapsulated by the six cyano groups with an $\text{Ag}\cdots\text{N}$ separation of 3.439(2) Å. The two phosphorus nuclei in **3** are crystallographically equivalent but magnetically non-equivalent since the molecule sits on a two-fold axis but lacks a centre of inversion. As a consequence of this symmetry the two phosphorus nuclei have identical chemical shifts, δ 11.2; however, $^2J(^{31}\text{P}^{31}\text{P})$ can be determined from slow MAS experiments. For **3** the space group is orthorhombic $Aba2$, $a = 15.142(1)$, $b = 24.917(2)$, $c = 10.2536(7)$ Å, $Z = 4$. The two phosphorus atoms are related by a crystallographically imposed two-fold axis. The nitrate group is chelated symmetrically to the Ag atom.

Bis(triphenylphosphine)silver nitrate has been widely used as a Lewis acid to synthesize numerous mixed-metal thiolate (or chalcogenide) clusters.¹ While continuing our studies of Group 11 metals with 1,1-dithiolate ligands, we have discovered that the anion, $[\text{Ag}_6(i\text{-mnt})_6]^{6-}$, [$i\text{-mnt} = \text{S}_2\text{CC}(\text{CN})_2^{2-}$] can be used as a 'cluster ligand' to build larger clusters stepwise by adding different stoichiometric amounts of $[\text{Ag}(\text{PPh}_3)_2]\text{NO}_3$, with ^{31}P NMR spectroscopy being a useful structural probe. Among structurally characterized compounds to date are the $[\text{Ag}_8(i\text{-mnt})_6(\text{PPh}_3)_4]^{4-}$ and $[\text{Ag}_9(i\text{-mnt})_6(\text{PPh}_3)_6]^{3-}$ cluster anions² in which two and three $[\text{Ag}(\text{PPh}_3)_2]^+$ cations are added to the octahedral $[\text{Ag}_6(i\text{-mnt})_6]^{6-}$ cluster core.

The interaction of the $[\text{Ag}(\text{PPh}_3)_2]^+$ cation with thiolate cluster anions is readily screened by $^{31}\text{P}\{-^1\text{H}\}$ NMR spectroscopy. The heteronuclear Ag-P coupling constant is extremely sensitive to the co-ordination environment around the silver centre.³ However, the coupling constants of the metal complexes normally cannot be resolved at ambient temperature due to the kinetic lability of the silver-phosphorus bond.⁴ Therefore low-temperature NMR experiments are required to obtain coupling-constant information. High-resolution solid-state cross polarization magic angle spinning (CP MAS) ^{31}P NMR spectroscopy is an excellent tool to obtain structural information.

In this paper the results of studies of $[\text{Ag}(\text{PPh}_3)_2]\text{NO}_3$ **1** by

high-resolution solid-state $^{31}\text{P}\{-^1\text{H}\}$ NMR spectroscopy are reported. An ABX, second-order solid-state NMR spectral pattern is uncovered with improved resolution compared to previously reported data.⁵ The crystal structures of the two new compounds $[\text{Ag}\{\text{P}(\text{CH}_2\text{CH}_2\text{CN})_3\}_2]\text{NO}_3$ **2** and $[\text{Ag}\{\text{P}(\text{C}_6\text{H}_4\text{Me-}m)_3\}_2]\text{NO}_3$ **3** and their solid-state $^{31}\text{P}\{-^1\text{H}\}$ NMR spectra also are described.

Experimental

Preparations.—*Bis(triphenylphosphine)silver(I) nitrate*, $[\text{Ag}(\text{PPh}_3)_2]\text{NO}_3$ **1**. Compound **1**, was synthesized following literature procedures.⁵ Single crystals were characterized by an X-ray cell-constant check and found to be identical to those reported.⁵

Bis[tris(2-cyanoethyl)phosphine]silver(I) nitrate, $[\text{Ag}\{\text{P}(\text{CH}_2\text{CH}_2\text{CN})_3\}_2]\text{NO}_3$ **2**. Silver nitrate (2.5 mmol) dissolved in hot acetonitrile (3 cm³) was added to a warm solution containing 2 equivalents of $\text{P}(\text{CH}_2\text{CH}_2\text{CN})_3$ dissolved in warm ethanol (50 cm³). The warm clear solutions were allowed to cool slowly in the dark to give well formed colourless crystals, yield 85%. IR (Nujol mull): $\nu(\text{CN})$ 2240s cm⁻¹ (Found: C, 38.35; H, 4.60; N, 17.10. Calc. for $\text{C}_{18}\text{H}_{24}\text{AgN}_7\text{O}_3\text{P}_2$: C, 38.85; H, 4.30; N, 17.60%), m.p. 123 °C.

Bis[tris(m-tolyl)phosphine]silver(I) nitrate, $[\text{Ag}\{\text{P}(\text{C}_6\text{H}_4\text{Me-}m)_3\}_2]\text{NO}_3$ **3**. The preparation followed the method used for compound **2** giving colourless crystals in 80% yield (Found: C, 64.55; H, 5.45; N, 1.85. Calc. for $\text{C}_{42}\text{H}_{42}\text{AgNO}_3\text{P}_2$: C, 64.80; H, 5.40; N, 1.80%), m.p. 130 °C.

† Supplementary data available: see Instructions for Authors, *J. Chem. Soc., Dalton Trans.*, 1995, Issue 1, pp. xxv-xxx.

Table 1 Crystallographic data

Complex	2	3
Empirical formula	C ₁₈ H ₂₄ AgN ₇ O ₃ P ₂	C ₄₂ H ₄₂ AgNO ₃ P ₂
<i>M</i>	556.25	778.63
Crystal system	Trigonal	Orthorhombic
Space group	<i>R</i> $\bar{3}c$	<i>Aba</i> 2
<i>a</i> /Å	12.204(2)	15.142(1)
<i>b</i> /Å	12.204(2)	24.917(2)
<i>c</i> /Å	26.418(5)	10.2536(7)
<i>U</i> /Å ³	3407.5(10)	3868.6(4)
<i>Z</i>	6	4
<i>D_c</i> /Mg m ⁻³	1.626	1.337
μ /mm ⁻¹	1.063	0.6327
<i>F</i> (000)	1692	1608
Crystal size/mm	0.6 × 0.5 × 0.4	0.15 × 0.22 × 0.4
Scan type	ω	ω -2 θ
Maximum 2 θ /°	50.04	46
Reflections collected	3920	2880
Independent reflections	678 (<i>R</i> _{int} , 0.0365)	2676
Refinement method	Full-matrix least squares on <i>F</i> ²	Full-matrix least squares
Data, restraints, parameters	678, 0, 55	2327, 0, 222
Goodness-of-fit ^a	1.130 (on <i>F</i> ²)	1.218 (on <i>F</i>)
Final <i>R</i> ^b indices [<i>I</i> > 2 σ (<i>I</i>)]	<i>R</i> 1 = 0.0242, <i>wR</i> 2 = 0.0642	<i>R</i> 1 = 0.023 11, <i>wR</i> = 0.031 82
(all data)	<i>R</i> 1 = 0.0251, <i>wR</i> 2 = 0.0650	
Largest difference peak and hole/e Å ⁻³	0.340, -0.315	0.31, -0.41

^a $[\sum(w||F_o| - |F_c||)^2]/(M - N)^{1/2}$, where *M* is the number of reflections and *N* the number of parameters refined. ^b *R*1 = $\sum||F_o| - |F_c||/\sum|F_o|$, *wR*2 = $\{\sum[w(F_o^2 - F_c^2)^2]/\sum(wF_o^4)\}^{1/2}$, *wR* = $\{\sum[w(F_o - F_c)^2]/\sum(wF_o^2)\}^{1/2}$.

Table 2 Atomic coordinates (× 10⁴) for [Ag{P(CH₂CH₂CN)₃}₂]-NO₃ 2

Atom	<i>x</i>	<i>y</i>	<i>z</i>
Ag	0	0	0
P	0	0	902(1)
C(1)	1491(2)	312(2)	1191(1)
C(2)	2672(2)	1368(2)	934(1)
C(3)	2911(2)	1006(2)	437(1)
N(1)	3099(2)	712(2)	54(1)
N(2)	0	0	2500
O(1)	0	974(5)	2500
O(1a)	950(6)	950(6)	2500

Spectroscopy.—Infrared spectra were recorded on a Perkin-Elmer 783 spectrophotometer, and solution ³¹P-¹H NMR spectra on a Varian XL-200 spectrometer using an internal deuterium lock. High-resolution solid-state NMR results were obtained on a Bruker MSL-300 spectrometer operated at 121.5 MHz for ³¹P. The samples were packed into a 7 mm zirconium oxide rotor. A Bruker CP MAS broad-band probe was used. The 90° pulse for ³¹P was 5 μ s and the cycle time was 60 s. The homogeneity of the static magnetic field was checked by ¹³C CP MAS NMR spectroscopy of adamantane. A linewidth of 1.8 Hz at half-maximum height was obtained. The two-dimensional *J*-resolved ³¹P spectrum was obtained using the pulse sequence CP-(*t*₁/2)-180°-(*t*₁/2)-acquisition, with an eight-pulse-phases⁶ cycle, and the increment of *t*₁ was synchronized with the rotation period of the sample. All phosphorus chemical shifts are referenced to external 85% H₃PO₄(aq).

Structure Determinations.—Colourless crystals of [Ag{P(CH₂CH₂CN)₃}₂]-NO₃ 2 and [Ag{P(C₆H₄Me-*m*)₃}₂]-NO₃ 3 suitable for X-ray diffraction analyses were grown from a MeCN solution and a CH₂Cl₂ solution, respectively, at ambient temperatures. Refined cell parameters were determined from the setting angles of 25 reflections with 20 < 2 θ < 30° for 2 and 30 < 2 θ < 32° for 3. For 2, data were obtained at room temperature using Mo-K α radiation (λ 0.710 73 Å) and a Nicolet R3/m diffractometer controlled by a Data General Nova 4 minicomputer. For compound 3, data were obtained at Notre

Dame on an Enraf-Nonius CAD4 diffractometer equipped with a graphite-crystal, incident-beam monochromator. Friedel pairs were collected.

The data were corrected for absorption, Lorentz and polarization effects. An empirical absorption correction based on a series of ψ scans was applied.

The Laue symmetry and systematic absences were consistent with the space group *R* $\bar{3}c$ for compound 2 and *Aba*2 for 3. The structure 2 was solved by standard Patterson and Fourier methods and refined using the SHELXL 93 crystallographic software package.^{7a} All non-hydrogen atoms were refined anisotropically. The hydrogen-atom positions were calculated by using fixed C-H bond lengths of 0.96 Å. The structure of 3 was solved by direct and Fourier methods performed on a VAX station 3200 computer using SDP/VAX.^{7b} The hydrogen-atom positions were refined isotropically and fixed for the anisotropic refinement. The isotropic thermal parameters were set to 1.1 times the *B*_{eq} of their bonded atoms. Refinement using the opposite chirality for the phasing produced a somewhat higher *R*₁ value of 0.030 82. The crystallographic details are given in Table 1. Atomic coordinates for structures 2 and 3 are listed in Tables 2 and 3, selected bond lengths and angles in Tables 4 and 5.

Results and Discussion

Structures.—The X-ray diffraction study demonstrates that the crystal structure of compound 1, [Ag(PPh₃)₂]-NO₃, which crystallizes in the space group *P* $\bar{1}$, is identical to that reported previously.⁵ Although the two distinct Ag-P bond lengths are essentially identical [2.443(1) and 2.440(1) Å], the solid-state ³¹P NMR results (see below) indicate that the two phosphorus nuclei have different isotropic chemical shifts (Table 7) and are thus crystallographically non-equivalent, in agreement with the X-ray results.

A thermal ellipsoid drawing of the structure of compound 2 is shown in Fig. 1. Both the Ag and the P atoms are located on a three-fold rotational axis with the Ag at the inversion centre. The Ag-P distance is 2.3832(9) Å. The conformation of the tris(2-cyanoethyl)phosphine (tcep) ligands in structure 2 is like the ribs of an umbrella. The silver atom is encapsulated by the six CN groups with an Ag...N separation of 3.439(2) Å. There

Table 3 Positional parameters for $[\text{Ag}\{\text{P}(\text{C}_6\text{H}_4\text{Me-}m)_3\}_2]\text{NO}_3 \cdot 3$

Atom	x	y	z
Ag	0.500	0.500	0.500
P	0.495 30(4)	0.590 39(3)	0.584 11(7)
O(1)	0.429 5(2)	0.502 14(7)	0.277 8(3)
O(2)	0.500	0.500	0.096 1(5)
N	0.500	0.500	0.215 2(5)
C(1)	0.589 7(2)	0.609 4(1)	0.683 7(2)
C(2)	0.617 6(2)	0.572 3(1)	0.778 2(3)
C(3)	0.691 0(2)	0.583 3(1)	0.855 8(3)
C(4)	0.735 2(2)	0.630 7(1)	0.838 6(3)
C(5)	0.709 0(2)	0.667 1(1)	0.744 2(3)
C(6)	0.636 3(2)	0.656 4(1)	0.667 4(3)
C(7)	0.720 9(3)	0.542 1(1)	0.956 6(3)
C(8)	0.489 1(1)	0.641 3(1)	0.456 7(3)
C(9)	0.524 9(2)	0.628 3(1)	0.336 3(3)
C(10)	0.520 0(2)	0.663 9(1)	0.230 9(3)
C(11)	0.479 0(2)	0.712 3(1)	0.250 1(3)
C(12)	0.444 0(2)	0.725 9(1)	0.370 5(3)
C(13)	0.448 8(2)	0.690 7(1)	0.471 8(3)
C(14)	0.557 0(3)	0.647 2(2)	0.102 8(4)
C(15)	0.398 7(2)	0.603 1(1)	0.684 8(3)
C(16)	0.396 7(2)	0.641 7(1)	0.781 7(3)
C(17)	0.319 1(2)	0.652 2(1)	0.850 9(3)
C(18)	0.244 9(2)	0.622 7(1)	0.819 4(3)
C(19)	0.246 3(2)	0.584 2(1)	0.723 9(4)
C(20)	0.323 4(2)	0.574 0(1)	0.657 5(3)
C(21)	0.317 3(2)	0.695 3(2)	0.955 3(4)

is no significant $\text{Ag} \cdots \text{NC}$ interaction, which is consistent with the IR spectrum wherein the position of the $\nu(\text{CN})$ band is the same as found for the free phosphine, 2240 cm^{-1} . The cation has S_6 point-group symmetry. The nitrate ion is disordered with the N atom located on the crystallographically imposed three-fold symmetry axis. The P–Ag–P angle is 180° . The torsional angle P–C–C–N is $71.4(1)^\circ$. Based on the X-ray data, the cone angle of the tcep ligand, measured following Tolman's approach,⁸ using a computer-generated space-filling model, is 175° .

Unlike bis(phosphine)gold(II) complexes which tend to be linear, two-co-ordinate species, the silver analogues are not readily obtained. In general, only very large and bulky tertiary phosphines form linear, two-co-ordinate complexes.⁹ Larger, less-bulky tertiary phosphines tend to form non-linear species¹⁰ with stronger anion co-ordination.¹¹ Compound **2** is only the second example of a structurally characterized, mononuclear bis(phosphine)silver(I) complex having a strictly linear geometry. In the previous example $[\text{Ag}\{\text{P}(\text{mes})_3\}_2]\text{PF}_6$ ($\text{mes} = \text{C}_6\text{H}_2\text{Me}_3\text{-}2,4,6$) the ligand cone angle is 203° .^{9a} The 0.08 \AA difference between the Ag–P distances in these two linear molecules [$2.461(6)$ versus $2.383(1) \text{ \AA}$ for **2**] must be due to differences in the electronic and steric properties of the phosphine ligands.

The tcep ligand has long been recognized for its unusual character. It is a better π acid¹² than the trialkylphosphines and is stable toward oxidation by O_2 . It has been reported that its cone angle is 132° .¹³ Here it is 175° . Although the Tolman cone angle is the most frequently employed measure of the steric size of phosphines and related ligands, the limitations of this approach are well recognized in that the cone angles may differ substantially with changes in the conformation of the ligands.¹⁴ This example shows that the cone angle changes dramatically as the ligand conformation changes.

Several metal complexes of tcep have been characterized structurally (Table 6). The structures of the tcep ligands are found in the umbrella and inverted-umbrella conformation, and anywhere in between. This is due to the mobility of this ligand and is evident from the torsional angles. (All three torsional angles of the ligand are in the same range in compounds in which the umbrella or inverted-umbrella conformations are observed.) Only two compounds with the

Table 4 Selected bond lengths (\AA) and angles ($^\circ$) for $[\text{Ag}\{\text{P}(\text{CH}_2\text{CH}_2\text{-CN})_3\}_2]\text{NO}_3 \cdot 2$

Ag–P	2.3832(9)	C(1)–C(2)	1.531(3)
P–C(1)	1.829(2)	C(3)–N(1)	1.136(3)
C(2)–C(3)	1.460(3)		
P ^I –Ag–P	180.0	C(1 ^{II})–P–C(1)	103.77(7)
C(1)–P–Ag	114.70(6)	C(2)–C(1)–P	114.16(13)
C(3)–C(2)–C(1)	113.0(2)	N(1)–C(3)–C(2)	179.0(2)

Symmetry transformations used to generate equivalent atoms: I – x, –y, –z; II –y, x – y, z.

Table 5 Selected bond lengths (\AA) and angles ($^\circ$) for $[\text{Ag}\{\text{P}(\text{C}_6\text{H}_4\text{Me-}m)_3\}_2]\text{NO}_3 \cdot 3$

Ag–P	2.4128(8)	Ag–O(1)	2.516(3)
P–C(1)	1.819(2)	P–C(8)	1.824(3)
P–C(15)	1.818(3)	O(1)–N	1.246(4)
O(2)–N	1.222(7)		
P–Ag–P'	138.11(2)	P–Ag–O(1)	106.94(5)
P–Ag–O(1')	110.85(5)	O(1)–Ag–O(1')	50.25(9)
Ag–P–C(1)	114.88(8)	Ag–P–C(8)	113.28(9)
Ag–P–C(15)	112.94(9)	Ag–O(1)–N	95.9(2)
O(1)–N–O(1')	118.0(4)	O(1)–N–O(2)	121.0(2)

tcep ligands in an umbrella shape have been structurally characterized (Table 6). They are isostructural and both have the metal atom (Au and Ag) encapsulated. No others are linearly two-co-ordinated species.

The structure determination of compound **3** (Fig. 2) confirms the 2:1 stoichiometry of the $[\text{Ag}\{\text{P}(\text{C}_6\text{H}_4\text{Me-}m)_3\}_2]^+$ fragment, with the nitrate group symmetrically chelating to the silver atom. The nitrate group and the silver atom are in the same plane with an Ag–O distance of $2.516(3) \text{ \AA}$. The Ag, N and O(2) atoms lie on a crystallographic two-fold axis. The O–Ag–O' angle is $50.25(9)^\circ$. The two phosphorus atoms are related by the crystallographically imposed two-fold axis. The Ag–P distance is $2.4128(8) \text{ \AA}$ and the P–Ag–P' angle is $138.11(2)^\circ$.

CP MAS ^{31}P NMR.—Although the crystal structure of $[\text{Ag}(\text{PPh}_3)_2]\text{NO}_3$ **1** determined by us is the same as that reported by Healy and co-workers,⁵ a total of sixteen peaks were resolved in our study of this ABX spin system (Fig. 3). The spectrum indicates that the two phosphorus nuclei are non-equivalent, δ_A 9.50 and δ_B 7.67, and spin–spin coupled to each other, $^2J(^{31}\text{P}_A\text{-}^{31}\text{P}_B) = 125 \text{ Hz}$. In addition, each of the four peaks of the AB portion of the spin system is split by spin–spin coupling to ^{107}Ag (spin $\frac{1}{2}$, natural abundance 51.82%) and ^{109}Ag (spin $\frac{1}{2}$, natural abundance 48.18%). Spectral analysis yields: $^1J(^{107}\text{Ag}\text{-}^{31}\text{P}) = 467 \pm 6$ and $^1J(^{109}\text{Ag}\text{-}^{31}\text{P}) = 524 \pm 6 \text{ Hz}$. As expected, the ratio $^1J(^{107}\text{Ag}\text{-}^{31}\text{P}):^1J(^{109}\text{Ag}\text{-}^{31}\text{P}) = 0.89:1$ is in good agreement with the magnetogyric ratios $\gamma(^{107}\text{Ag}):^{109}\text{Ag} = 0.870:1$. In solution, the two phosphorus nuclei of **1** have the same phosphorus chemical shift (δ 10.75) and are thus chemically equivalent. Owing to rapid intermolecular ligand exchange in solution at the probe temperature, it is necessary to acquire spectra at low temperatures in order to resolve splittings due to silver–phosphorus spin–spin coupling. In CDCl_3 solution at -60°C , $^1J(^{107}\text{Ag}\text{-}^{31}\text{P}) = 466 \pm 1$ and $^1J(^{109}\text{Ag}\text{-}^{31}\text{P}) = 534 \pm 1 \text{ Hz}$. Note that the ratio is now 0.873:1 and closer to the theoretical value of 0.870:1 because of the smaller errors associated with the solution-state measurement.

Since the $^2J(\text{PP})$ values (Table 7) are comparable with, but smaller than, the chemical shift difference between the two P atoms, the CP MAS spectrum (Fig. 3) shows a second-order

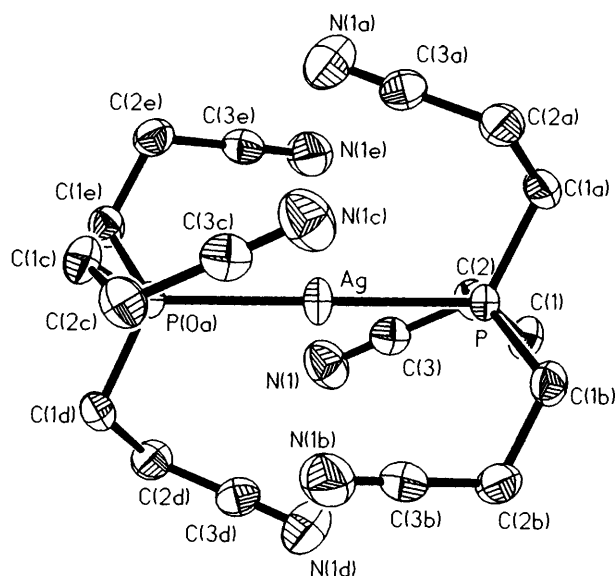


Fig. 1 Thermal ellipsoid drawing (50% probability) of $[\text{Ag}(\text{P}(\text{CH}_2\text{CH}_2\text{CN})_3)_2]\text{NO}_3$

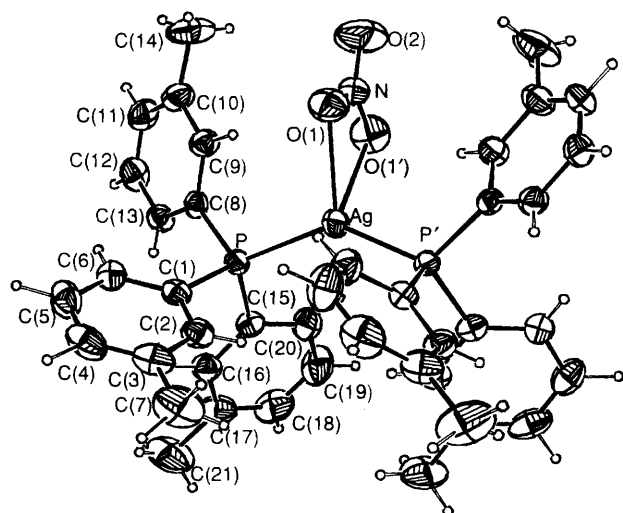


Fig. 2 Thermal ellipsoid drawing (50% probability) of $[\text{Ag}(\text{P}(\text{C}_6\text{H}_4\text{Me-}m)_3)_2]\text{NO}_3$

effect with irregular intensities for each ^{31}P doublet. The two ^{31}P atoms are close to each other, thus there is a dipole-dipole interaction between them. Such interactions can be averaged to zero by fast spinning at the magic angle. The spectral pattern depends on the spinning rate. When the instantaneous difference in the chemical shifts of the two homonuclear dipole-coupled nuclei is comparable to the coupling between them the system shows an unusual spin-rate dependence. Such behaviour has been extensively studied.^{6,26-34} Fig. 4 shows the CP MAS spectra of the sample at different spinning rates. It can be seen that the position of each peak in the isotropic region does not change with the spin rate but the peak intensities vary dramatically from sideband to sideband. The total MAS spectrum is the summation of the isotropic peaks and all the spinning sidebands (Fig. 5). It can be seen that the anomalous features for individual sidebands disappear and a symmetric spectrum is obtained at all spin rates. It was found in a previous study that the CP MAS ^{31}P NMR spectra of *cis*-1,2-bis-(diphenylphosphino)ethylene and *trans*- $[\text{Rh}(\text{CO})\text{Cl}(\text{PPh}_3)_2]$ have similar features.³²

The above analysis is confirmed by the ^{31}P CP MAS

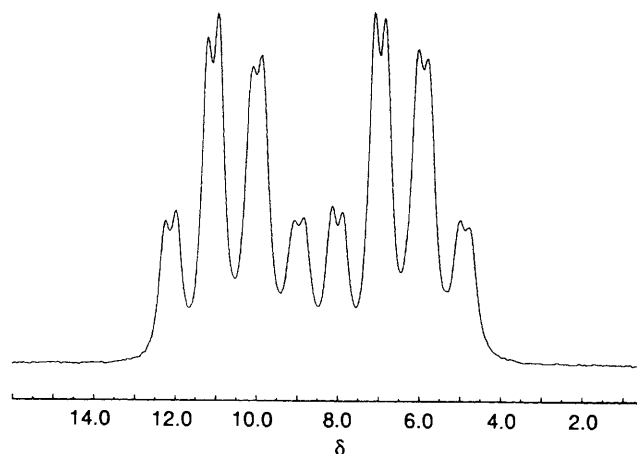


Fig. 3 The CP MAS ^{31}P NMR spectrum of $[\text{Ag}(\text{PPh}_3)_2]\text{NO}_3$, at a rotor spinning rate of 4.0 kHz

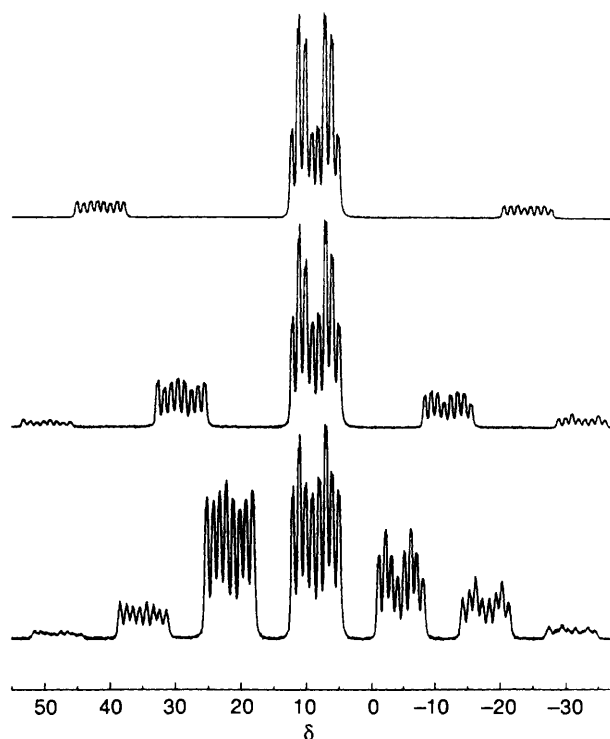


Fig. 4 The CP MAS ^{31}P NMR spectra of $[\text{Ag}(\text{PPh}_3)_2]\text{NO}_3$ at different rotor spinning rates: top, 4.0; middle, 2.5; bottom, 1.6 kHz

homonuclear J -resolved two-dimensional spectrum shown in Fig. 6. In this spectrum the two non-equivalent ^{31}P atoms with different isotropic chemical shifts are not only spin-spin coupled with the silver nuclei resulting in four peaks in the F2 dimension, but are also spin-spin coupled to each other resulting in peak pairs in the F1 dimension. The $^1J(^{107,109}\text{Ag}^{31}\text{P})$ and $^2J(^{31}\text{P}^{31}\text{P})$ data extracted match the results calculated above (Table 7).

Fig. 7 is the static CP ^{31}P NMR spectrum of $[\text{Ag}(\text{PPh}_3)_2]\text{NO}_3$. The spectral width is about 7 kHz, which is much larger than the dipole-dipole interaction estimated to be about 212 Hz based on a distance of 4.54 Å between P atoms. The difference between the two non-equivalent P atoms can be neglected because the difference between the isotropic chemical shifts of two ^{31}P atoms is about 200 Hz. It is assumed that the chemical shift tensors of the two ^{31}P atoms are approximately the same. In solution the two ^{31}P atoms are equivalent. The three phenyl rings on each P are also equivalent since there is

Table 6 Metal complexes containing the P(CH₂CH₂CN)₃ (tcep) ligand

Compound	Torsional angle ^{a/o}	Conformation of ligand	Ref.
[Ag(tcep) ₂]NO ₃	71.4	Umbrella	This work
[Au(tcep) ₂]Cl	71.4	Umbrella	15
[Ni(NCS) ₄ (tcep) ₂] ²⁻	174.6, 173.2, 78.9	<i>b</i>	16
[Ni(NCS) ₂ (tcep) ₂] ^a	178.6, 175.8, 37.4	<i>b</i>	17
b^c	176.4, 167.5, 88.4	<i>b</i>	
	179.1, 179.0, 67.2	<i>b</i>	17
	169.8, 84.4, 60.6	<i>b</i>	
c^c	180.0, 171.1, 70.6	<i>b</i>	17
[{HgCl ₂ (tcep)} _n]	171.3, 170.2, 74.5	<i>b</i>	18
[Cr(CO) ₅ (tcep)]	176.8, 169.3, 72.5	<i>b</i>	19
[Mo(CO) ₅ (tcep)]	176.8, 169.3, 72.5	<i>b</i>	19
[NiBr ₂ (tcep) ₂]	179.8, 172.0, 66.3	<i>b</i>	20
[HgCl ₂ (tcep) ₂]	171.3, 160.8, 49.0	<i>b</i>	21
	151.3, 120.8, 49.1	<i>b</i>	
[AuCl(tcep)] ^d	178.9, 70.9, 61.6	<i>b</i>	22
e^c	176.9, 169.9, 66.8	<i>b</i>	22
[Ni ₄ (CO) ₆ (tcep) ₄]	179.5, 179.5, 179.5	Inverted umbrella	23
	175.4, 167.9, 87.2	<i>b</i>	
[HgBr ₂ (tcep) ₂]·Me ₂ CO	176.1, 175.1, 172.6	Inverted umbrella	18
	177.2, 174.6, 173.6	Inverted umbrella	
<i>trans</i> -[PtCl ₂ (tcep) ₂]	179.0, 171.0, 166.5	Inverted umbrella	15
[Au(S ₂ COEt)(tcep) ₂]	177.9, 166.4, 62.2	<i>b</i>	24
	177.8, 176.8, 149.7	Inverted umbrella	
[Mo ₂ Cl ₄ (tcep) ₂ (NCMe)]·MeCN	174.7, 173.9, 165.4	Inverted umbrella	25

^a P-C-C-CN. Only the absolute value of the angle was used. Crystallographic errors are generally ±0.1°. ^b Between the umbrella and inverted umbrella. ^c Polymorph.

Table 7 Phosphorus-31 CP MAS NMR parameters

Compound	δ ± 0.05	¹ J(^{107,109} Ag ³¹ P) ± 6 Hz	² J(³¹ P ³¹ P) ± 6 Hz
[Ag(PPh ₃) ₂]NO ₃	9.50, 7.67	467, 524	125
[Ag{P(CH ₂ CH ₂ CN) ₃ } ₂]NO ₃	-9.56	496, 564	
[Ag{P(C ₆ H ₄ Me- <i>m</i>) ₃ } ₂]NO ₃ *	11.2	453, 517	140

* See ref. 35.

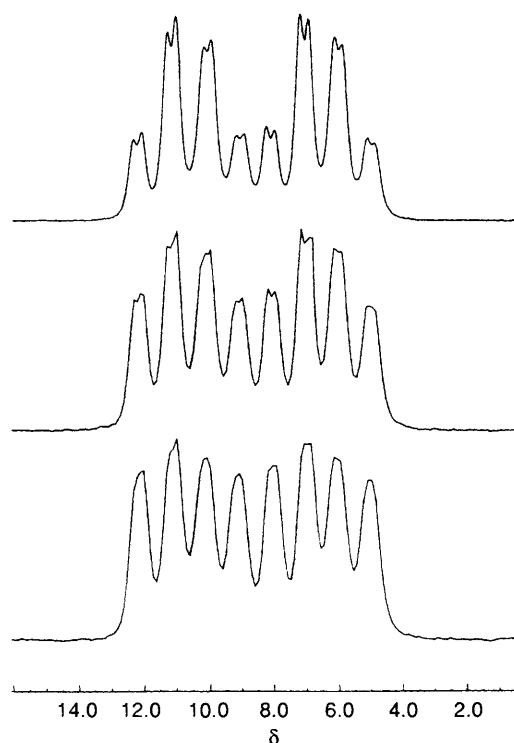


Fig. 5 Total MAS spectra of [Ag(PPh₃)₂]NO₃ at different rotor spinning rates. Details as in Fig. 4

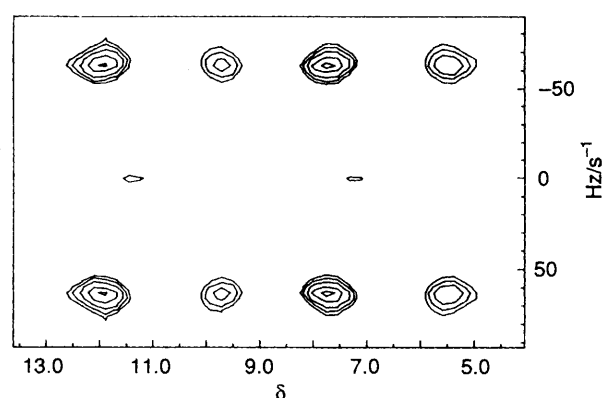


Fig. 6 The ³¹P CP MAS homonuclear *J*-resolved two-dimensional spectrum of [Ag(PPh₃)₂]NO₃

local *C*₃ symmetry which goes through the P-Ag axis. In the solid state, tensor fitting shows that δ₁₁ 34.0 ± 1.0, δ₂₂ 17.0 ± 1.0 and δ₃₃ -24.5 ± 1.0. This indicates that the local *C*₃ symmetry is distorted and the three phenyl rings on each P are not exactly related by a *C*₃ axis. Based upon the axial shape of the spectrum and previous studies, it is reasonable to assume that δ₃₃ aligns nearly parallel to the P-Ag axis while δ₁₁ and δ₂₂ are perpendicular to this axis. However, we do not have data which provides this information.

Initially we attempted to understand why our ³¹P NMR spectrum of compound 1 is different from that reported previously by Healy and co-workers.⁵ Their published spectrum appeared inconsistent with the *P* $\bar{1}$ symmetry, *Z* = 2,

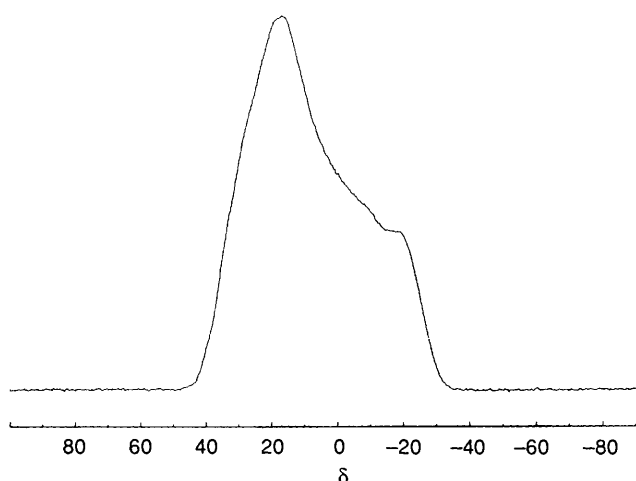


Fig. 7 The ^{31}P NMR static spectrum of $[\text{Ag}(\text{PPh}_3)_2]\text{NO}_3$

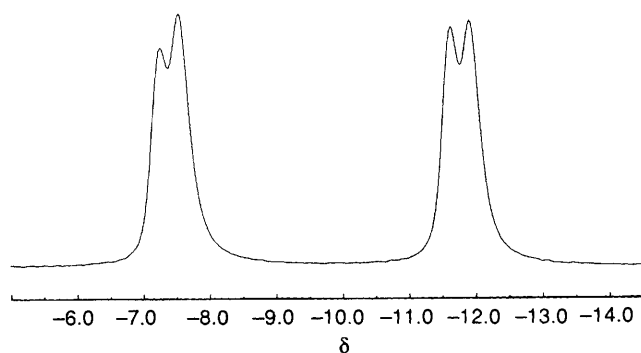


Fig. 8 The CP MAS ^{31}P NMR spectrum of $[\text{Ag}\{\text{P}(\text{CH}_2\text{CH}_2\text{CN})_3\}_2]\text{NO}_3$

of the crystalline material. Besides signal resolution, it seemed possible to us that a higher symmetry might have been introduced by sample handling. A symmetrical structure is obtained for compound **3** which shows a CP MAS ^{31}P NMR spectrum similar to that reported by Healy and co-workers.⁵ Thus we heated and cooled our sample in a vain attempt to change the NMR spectrum. However, by introducing a line broadening of 100 Hz, the spectrum of ref. 5 can be reproduced. Hence spectral resolution, as suggested by Healy and co-workers⁵ is the origin of the differences observed.

Fig. 8 presents the CP MAS spectrum of $[\text{Ag}\{\text{P}(\text{CH}_2\text{CH}_2\text{CN})_3\}_2]\text{NO}_3$ upon spinning with a rotor speed of 3.5 kHz. The two P atoms, which are related to each other by the inversion centre, are crystallographically and magnetically equivalent with a linear P–Ag–P bonding. Therefore, the dipole–dipole interaction between the two P atoms is small due to their relatively large separation and is averaged to zero by fast sample spinning. Only the effect of the presence of two silver isotopes with the spin–spin coupling between ^{31}P and ^{109}Ag and ^{107}Ag is observed. The inner peak pair of the doublet is the spin–spin coupling of $^1J(^{31}\text{P}^{107}\text{Ag}) = 496 \pm 6$ Hz and the outer peak pair is the spin–spin coupling of $^1J(^{31}\text{P}^{109}\text{Ag}) = 564 \pm 6$ Hz. The isotropic chemical shift of the ^{31}P is $\delta = -9.56$. The static spectrum of this compound shows an axially symmetric chemical shift tensor pattern with $\delta_{\perp} = -7.2 \pm 1.0$ and $\delta_{\parallel} = -14.0 \pm 1.0$ by tensor fitting; δ_{\perp} is perpendicular to the P–Ag–P axis and δ_{\parallel} aligns on the P–Ag–P axis.

The two phosphorus atoms of compound **3** are crystallographically equivalent but magnetically non-equivalent. They are related by a two-fold rotation axis in the space group Aba_2 . The solid-state ^{31}P NMR spectra exhibit interesting rotor spinning-frequency-dependent line shapes with details which are reported elsewhere.³⁵

The solid-state NMR results reported here agree with earlier studies which show that the coupling constant, $J(\text{AgP})$ increases with decreasing Ag–P distance, increasing P–Ag–P angle, and decreasing nucleophilicity of the co-ordinating atom in the counter ion.³⁶ The coupling constant difference between compounds **1** and **2** suggests that there is more Ag 5s orbital involvement in compound **2** compared with **1**. Furthermore, the sensitivity of CP MAS NMR data to subtle structural features observed in Ag–P complexes in general is apparent from this work.

Acknowledgements

Financial support from the Robert A. Welch Foundation and the National Science Foundation, CHE 9300107, is appreciated by J. P. F. Work in Canada was financially supported by the Natural Sciences and Engineering Research Council for which R. E. W. is grateful.

References

- 1 A. Müller, E. Diemann, R. Josters and H. Bögge, *Angew. Chem., Int. Ed. Engl.*, 1981, **20**, 934; I. G. Dance, *Polyhedron*, 1986, **5**, 1037; X. Wu, P. Chen, S. Du, N. Zhu and J. Lu, *J. Cluster. Sci.*, 1994, **5**, 265; D. Coucouvanis, F. J. Hollander and M. Leitheiser, *Inorg. Chem.*, 1977, **16**, 1615; D. Coucouvanis and F. J. Hollander, *Inorg. Chem.*, 1974, **13**, 2381; D. Coucouvanis, N. C. Baenziger and S. M. Johnson, *Inorg. Chem.*, 1974, **13**, 1191.
- 2 C. W. Liu and J. P. Fackler, jun., unpublished work.
- 3 D. K. Johnson, P. S. Pregosin and L. M. Venanzi, *Helv. Chim. Acta*, 1976, **59**, 2691; M. Barrow, H.-B. Bürgi, D. K. Johnson and L. M. Venanzi, *J. Am. Chem. Soc.*, 1976, **98**, 2356.
- 4 E. L. Muetterties and C. W. Alegranti, *J. Am. Chem. Soc.*, 1972, **94**, 6386.
- 5 P. F. Barron, J. C. Dayson, P. C. Healy, L. M. Engelhardt, B. W. Skelton and A. White, *J. Chem. Soc., Dalton Trans.*, 1986, 1965.
- 6 K. Eichele, G. Wu and R. E. Wasylshen, *J. Magn. Reson. A*, 1993, **101**, 157.
- 7 (a) G. M. Sheldrick, SHELXL 93, University of Göttingen, 1993; (b) B. A. Frenz, *Computing in Crystallography*, eds. H. Schenk, R. Olthof-Hazelkamp, H. van Königsveld and G. C. Bussi, Delft University Press, Delft, 1978, pp. 64–71.
- 8 C. A. Tolman, *Chem. Rev.*, 1977, **77**, 313.
- 9 (a) E. C. Alyea, G. Ferguson and A. Smogyvari, *Inorg. Chem.*, 1982, **21**, 1369; (b) H. H. Karsch and U. Schubert, *Z. Naturforsch., Teil B*, 1982, **37**, 186.
- 10 R. J. Restivo, A. Costin and G. Ferguson, *Can. J. Chem.*, 1975, **53**, 1949; S. M. Socol, R. A. Jacobson and J. G. Verkade, *Inorg. Chem.*, 1984, **23**, 88.
- 11 A. Baiada, F. H. Jardine and R. D. Willett, *Inorg. Chem.*, 1990, **29**, 3042.
- 12 C. A. Streuli, *Anal. Chem.*, 1960, **32**, 985.
- 13 Md. M. Rahman, H. Y. Liu, A. Prock and W. P. Giering, *Organometallics*, 1987, **6**, 650; Md. M. Rahman, H. Y. Liu, K. Eriks, A. Prock and W. P. Giering, *Organometallics*, 1989, **8**, 1.
- 14 D. White and N. J. Coville, *Adv. Organomet. Chem.*, 1994, **36**, 95.
- 15 Md. N. I. Khan, C. King, J. P. Fackler, jun., and R. E. P. Wippeny, *Inorg. Chem.*, 1993, **32**, 2502.
- 16 B. M. Foxman and H. Mazurek, *Inorg. Chem.*, 1978, **18**, 113.
- 17 B. M. Foxman, P. L. Goldberg and H. Mazurek, *Inorg. Chem.*, 1981, **20**, 4368.
- 18 N. A. Bell, M. Goldstein, L. A. March and I. W. Nowell, *J. Chem. Soc., Dalton Trans.*, 1984, 1621.
- 19 F. A. Cotton, D. J. Darensbourg and W. H. Ilsley, *Inorg. Chem.*, 1981, **20**, 578.
- 20 K. Cheng and B. M. Foxman, *J. Am. Chem. Soc.*, 1977, **99**, 8102.
- 21 N. A. Bell, L. A. March and I. W. Nowell, *Inorg. Chim. Acta*, 1989, **156**, 195.
- 22 J. P. Fackler, jun., R. J. Staples, Md. N. I. Khan and R. E. P. Wippeny, *Acta Crystallogr., Sect. C*, 1994, **50**, 1020.
- 23 M. J. Bennett, F. A. Cotton and B. H. C. Winguist, *J. Am. Chem. Soc.*, 1967, **89**, 5366.
- 24 Z. Assefa, R. J. Staples and J. P. Fackler, jun., *Inorg. Chem.*, 1994, **33**, 2790.
- 25 F. A. Cotton and E. Walke, unpublished work.
- 26 M. M. Maricq and J. S. Waugh, *J. Chem. Phys.*, 1979, **70**, 3300.

- 27 S. Hayashi and K. Hayamizu, *Chem. Phys. Lett.*, 1989, **161**, 158.
28 S. Hayashi and K. Hayamizu, *Chem. Phys.*, 1991, **157**, 381.
29 A. Kubo and C. A. McDowell, *J. Chem. Phys.*, 1990, **92**, 7156.
30 W. P. Power and R. E. Wasylishen, *Inorg. Chem.*, 1992, **31**, 2176.
31 E. Lindner, R. Fawzi, H. A. Mayer, K. Eichele and W. Hiller, *Organometallics*, 1992, **11**, 1033.
32 G. Wu and R. E. Wasylishen, *Inorg. Chem.*, 1992, **31**, 145; G. Wu, R. E. Wasylishen and R. D. Curtis, *Can. J. Chem.*, 1992, **70**, 863; G. Wu and R. E. Wasylishen, *J. Chem. Phys.*, 1993, **99**, 6321.
33 G. Szaloutai, J. Bakos, S. Aime and R. Gobtto, *Solid State Nuclear Magnetic Resonance*, 1993, **2**, 245.
34 G. Wu and R. E. Wasylishen, *J. Chem. Phys.*, 1993, **98**, 6138.
35 G. Wu, R. E. Wasylishen, H. J. Pan, C. W. Liu, J. P. Fackler, jun., and M. Y. Shang, *Magn. Reson. Chem.*, 1995, **33**, 734.
36 M. Barrow, H.-B. Bürgi, M. Camalli, F. Caruso, E. Fisher, L. M. Venanzi and L. Zambonelli, *Inorg. Chem.*, 1983, **22**, 2356.

Received 13th April 1995; Paper 5/02379C